

## Performance Attributes of Generalized Time-Frequency Representations with Double Diamond and Cone Shaped Kernels

Seho Oh and Robert J. Marks II  
 Department of Electrical Engr., FT-10  
 University of Washington  
 Seattle, WA 98195  
 (206) 543-2150

### Abstract

Zhao, Atlas and Marks (ZAM) have empirically shown that generalized time-frequency representations with cone shaped kernels display quite good time frequency representations in comparison to other approaches. The double diamond (DD) GTFR introduced in this paper is subsumed in the cone support, and also displays some remarkable performance attributes. The conventional sliding window spectrogram has a single diamond shape window support. In this paper, we analyze some specific properties of the DD and ZAM GTFR's and compare them to other TFR's. For stationary tone signals, both the DD and ZAM GTFR are shown asymptotically to produce results identical to that of the spectrogram. When a signal is subjected to white noise, the DD and ZAM GTFR's produces an unbiased estimate of the GTFR of the signal without noise. For GTFR's satisfying the marginals, the power spectral density of the noise, rather, is superimposed on the GTFR of the signal. The DD GTFR is shown to have superb mid frequency interference properties almost identical to that of the spectrogram. The temporal rise time of the DD GTFR is comparable that of the ZAM GTFR and Wigner distributions. The leakage properties of the DD GTFR can be significantly better than those of the ZAM GTFR, Wigner distribution and spectrogram.

### 1 Introduction

The *Generalized Time Frequency Representation* (GTFR) of Cohen [1, 2] is a powerful generalization of time frequency representations in which a number of important special cases are subsumed. These include the spectrogram, Wigner distribution, CW GTFR (Choi, Williams) [3, 4] and the ZAM GTFR (Zhao, Atlas and Marks) [5, 6].

In this paper, we introduce the double diamond (DD) GTFR and analytically establish some significant properties of the ZAM [5, 6, 10] and DD GTFR's. Specifically

1. *Spectrogram relation:* For the case of a superposition of a number of sinusoids, the DD and ZAM GTFR's asymptotically approach the spectrogram.
2. *Interference term:* The DD and ZAM GTFR are shown to significantly outperform the Wigner distribution in terms of interference suppression. Indeed, we will present important scenarios where the DD GTFR has interference characteristics that are nearly indistinguishable from those of the spectrogram.

A comparative illustration of five TFR's is shown in Figures 1 and 2 for two converging linear chirps. Interference can also be seen in the multi-on/off tone signal shown in a waterfall display in Figure 3 and in a gray level plot in Figure 4.

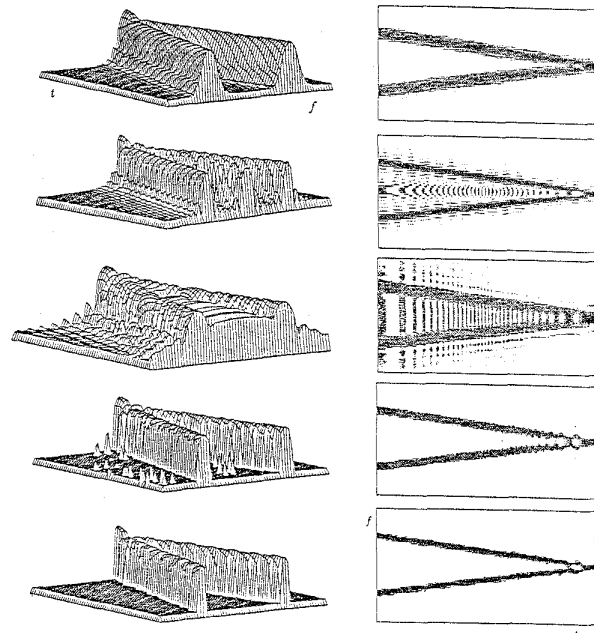


Figure 1: Five TFR's of two linearly converging chirps. Each has a 35dB spread from floor to peak. From top to bottom are the spectrogram, Wigner, CW, ZAM and DD GTFR's. Each TFR was computed using a Hanning window. Each used the same signal interval (128 points) for each spectral line. The spectrogram displays the desired V shape. The Wigner distribution contains an oscillating interference term midway between the frequencies. The CW GTFR spreads this interference while maintaining the marginals. The ZAM GTFR has higher interference than the DD GTFR.

Figure 2: Gray level plots of the TFR's in Figure 1.

3. *Frequency resolution:* Frequency resolution is measured by examining how close two stationary tones can be placed in frequency such that they are still distinguishable in the TFR. Due to the interference term, the Wigner distribution performs poorly in this regard and is therefore outperformed by the ZAM GTFR. As the TFR of choice for stationary signals, however, the spectrogram has even better frequency resolution. We will show, however, that the DD GTFR can have frequency resolution properties quite close to those of the spectrogram.

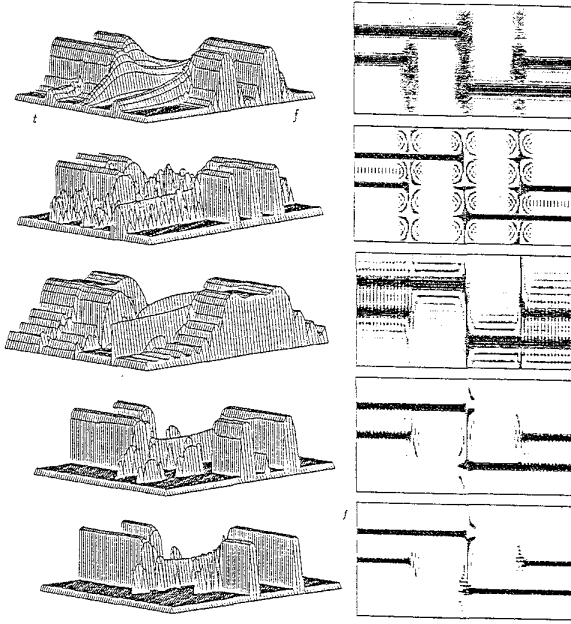


Figure 3: Five TFR's of a number of switched tones. The TFR's were computed as in Figure 1.

Figure 4: Gray level plots of the TFR's in Figure 3.

4. *Time resolution:* The ability of the TFR to make the transition in an instantaneous frequency change is an indication of the TFR's time resolution capability. We illustrate that the rise time for the DD and ZAM GTFR's can be close to that of the Wigner distributions. The ripple in the DD ZAM GTFR can be substantially smaller than that of the Wigner distribution. The DD GTFR, in particular, displays impressive ripple performance. Its response prior to point of transition is nearly zero. The spectrogram displays correspondingly poor time resolution performance. (See Figures 1-4).
5. *Noise sensitivity:* When a signal is corrupted by additive white noise, the DD and ZAM GTFR's displays an unbiased estimate of the corresponding GTRF of the noiseless signal. This is contrast to the Wigner distribution and spectrogram where the power spectral density of the noise is added to the result. Noise sensitivity is illustrated in Figure 5 for the TFR's of a sequence of four tones.

The DD and ZAM GTFR's are also real and shift-invariant. As is the case with the spectrogram, the DD and ZAM GTFR's do not obey the *marginals*, [1, 2] *i.e.* the integral projection onto the time axis of the ZAM GTFR does not result in the signal's instantaneous power, nor does the projection onto the frequency axis result in the power spectral density. Thus, unlike the Wigner-Ville and Choi-Williams distributions, the ZAM GTFR cannot be interpreted as a time-frequency density function for the signals. Recent results [12] suggest, however, that significantly higher resolution in both time and frequency can be bought with sacrifice of the marginals. The analytic and empirical results in this paper are further evidence of this proposition.

## 2 Characteristics of the DD and ZAM GTFR's

In this section, we derive some important performance attributes of the continuous time DD and ZAM GTFR and contrast them to the Wigner distribution and spectrogram. A summary of some of our conclusions is listed in Table 1. Other distributions and attributes will also be considered. We will, in each case, define the attribute and analyze the corresponding TFR performance.

### 2.1 The DD and ZAM GTFR's

The general continuous time formula of Cohen's GTFR class is

$$C(t, f; \phi) = \int_{-\infty}^{\infty} \int_{-\infty}^{\infty} \hat{\phi}(t-u; \tau) x\left(u + \frac{\tau}{2}\right) \times x^*\left(u - \frac{\tau}{2}\right) e^{-j2\pi f\tau} ds du \quad (1)$$

where  $\hat{\phi}(t; \tau)$  is the GTFR kernel.

The kernel function of the ZAM GTFR is

$$\hat{\phi}(\eta, \tau) = \rho(\tau) \Pi\left(\frac{t}{\tau}\right) \quad (2)$$

where  $\rho(\tau)$  is a windowing function and  $\Pi(t) = 1$  for  $|t| \leq \frac{1}{2}$  and is otherwise zero. For  $\rho(\tau) = 1/|\tau|$ , we have Cohen's Born-Jordan kernel [1, 2]. Tapers other than uniform have also been proposed [12].

If  $\rho(\tau)$  is identically zero for  $|\tau| > T$ , then cone shaped region of support of (2) is shown in Figure 6.

A DD GTFR has a kernel that is zero in the double diamond area illustrated in Figure 6. The support of the kernel is parameterized by  $T$ . The DD GTFR can be written as

$$C_{DD}(t, f; \phi) = \int \int_{(t, \tau) \in DD} \hat{\phi}(t-s; \tau) x\left(s + \frac{\tau}{2}\right) \times x^*\left(s - \frac{\tau}{2}\right) e^{-j2\pi f\tau} ds d\tau \quad (3)$$

where integration is over all  $(t, \tau)$  in the double diamond centered at  $t = s$ . As with the ZAM GTFR, the DD GTFR can be shown to be real when the kernel displays certain symmetry constraints [1]. As is the case with the ZAM GTFR, it can also be negative. Note that the DD kernel is subsumed in the cone.

In the next section, we show that the positive portion of both the ZAM and DD GTFR's approach the same response as that of the spectrogram for certain stationary signals. Note that by setting the negative portions of the ZAM GTFR to zero, we obtain the projection onto the nearest nonnegative function, *i.e.* we obtain the closest non-negative time frequency representation in the mean square sense.

### 2.2 Stationary Signal Time Response

For a number of stationary tones, both the DD and ZAM GTFR can approach a spectrogram as  $T$  increases. We will give a detail proof for the case of the ZAM GTFR.

Let  $C(t, f; \theta)$  be the ZAM GTFR with

$$\rho(\tau) = \frac{1}{T} \theta\left(\frac{\tau}{T}\right) \Pi\left(\frac{\tau}{2T}\right) \quad (4)$$

where  $\theta(u)$  is the normalized windowing function. Define

$$\Theta^{(1)}(\alpha) = \int_0^1 u \theta(u) e^{-j2\pi u \alpha} du \quad (5)$$

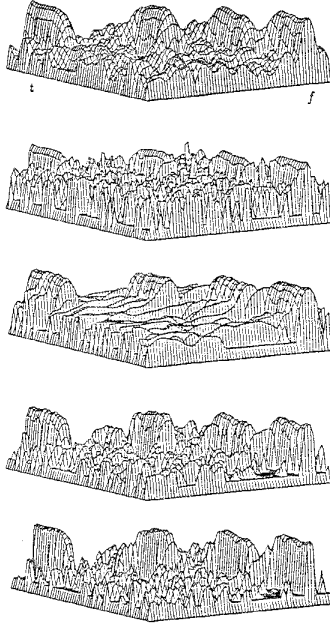


Figure 5: Five TFR's of a sequence of four tones in noise at a 3dB SNR. The manner of computation and display is the same as is described in the caption of Figure 1.

and

$$\Theta^{(2)}(\alpha) = \int_0^1 \theta(u) e^{-j2\pi u \alpha} du \quad (6)$$

For the ZAM GTFR,  $\rho(\tau) = 0$  for  $|\tau| > T$ , we can write (2) as,

$$C(t, f; \theta) = \frac{1}{T} \int_{-T}^T \int_{t-\frac{|r|}{2}}^{t+\frac{|r|}{2}} \theta\left(\frac{r}{T}\right) x\left(s + \frac{r}{2}\right) \times x^*\left(s - \frac{r}{2}\right) e^{-j2\pi f r} ds dr \quad (7)$$

We can now state the following property for stationary signals with a finite number of frequency components.

**Property 1** Assume that

$$x(t) = \sum_i X_i e^{j2\pi f_i t} \quad (8)$$

If  $\theta(u)$  is bounded and has finite energy, then, for both ZAM and DD GTFR's

$$\lim_{T \rightarrow \infty} \text{Pos}[C(t, f; \theta)] = A \sum_i |X_i|^2 \delta(f - f_i)$$

where  $A$  is determined by windowing. A proof for the ZAM GTFR is in Reference [11]

### 2.3 Interference Terms

A significant problem in many GTFR's is the appearance of unwanted interference terms. For two simultaneous frequencies, the interference term typically appears midway between the frequencies. As is illustrated in Figures 1-4, the DD and ZAM GTFR's reduce the interference terms significantly. Indeed, from the results of the previous section on the asymptotic equivalence of the DD and ZAM GTFR's to the spectrogram, we are guaranteed no interference terms midway between the frequency as  $T \rightarrow \infty$ .

	DD GTFR	ZAM GTFR	Spectrogram	Wigner
Asymptotically Spectrogram?	yes	yes	yes	no
Frequency Resolution	better	good	best	fair
Time Resolution:				
• leakage...	best	better	fair	good
• rise time...	better	best	fair	better
White Noise Bias?	no	no	yes	yes

Table 1: Summary of attributes of four time-frequency distributions. The text of the paper should be consulted for elaboration on the meaning of and the specific methods for determination of the entries.

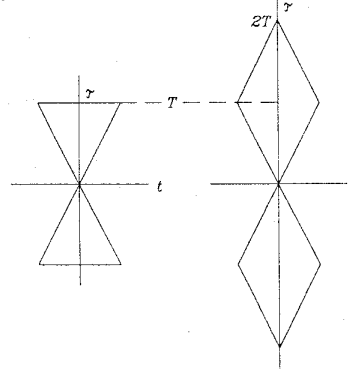


Figure 6: The cone (left) and double diamond (right) supports corresponding to a window duration of  $2T$ .

To explore the interference properties for intermediate values of  $T$ , assume the stationary signal in (8) has two terms

$$x(t) = X_1 e^{j2\pi f_1 t} + X_2 e^{j2\pi f_2 t} \quad (9)$$

For the ZAM GTFR, we can write

$$C(t, f; \rho) = \sum_i C_i^{(1)}(t, f; \rho) + \sum_{i,j} C_{ij}^{(2)}(t, f; \rho) \quad (10)$$

It follows that the interference term is [11]

$$C_{12}^{(2)} + C_{21}^{(2)} = \frac{2|X_1||X_2|}{\pi(f_1 - f_2)} \cos[2\pi\{(f_1 - f_2)t + (\psi_1 - \psi_2)\}] \times \text{Im}[\Theta^{(2)}\{(f - f_1)T\} - \Theta^{(2)}\{(f - f_2)T\}]$$

where the frequency midpoint is  $f = (f_1 + f_2)/2$ . The magnitude of the interference is the cosine's envelope,

$$\chi(\Delta f; T) = \frac{2|X_1||X_2|}{\pi\Delta f} |\text{Im}[\Theta^{(2)}(T\Delta f/2)]| \quad (11)$$

where  $\Delta f = |f_1 - f_2|$ .

We will now show that the interference term can decrease as  $\mathcal{O}(\{T\Delta f^2\}^{-1})$  for both the DD and ZAM GTFR's. We here consider only the ZAM GTFR. If the window,  $\theta(u)$ , is monotonically decreasing for  $0 \leq u \leq 1$ , then

$$\begin{aligned} \text{Im}[\Theta^{(2)}(f)] &= \int_0^1 \theta(u) \sin(2\pi f u) du \\ &\leq \theta(0) \int_0^{\frac{1}{2f}} \sin(2\pi f u) du \\ &= \frac{\theta(0)}{\pi f} \end{aligned} \quad (12)$$

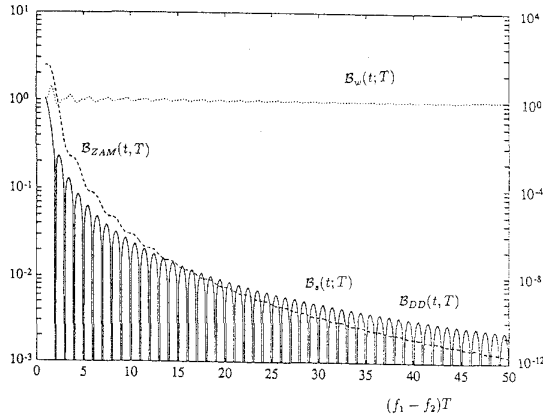


Figure 7: Interference measures for the Wigner distribution, ZAM GTFR, DD GTFR and spectrogram. The DD GTFR and spectrogram plots use the log scale on the right and are graphically indistinguishable. The ZAM GTFR and Wigner use log scale on the left.

from which we conclude  $|\text{Im}\{\Theta^{(2)}(f)\}| \leq |\theta(0)/(\pi f)|$ . Thus, from (11), we have the following interference bound for the ZAM GTFR.

$$\frac{\chi(\Delta f; T)}{|X_1||X_2|} \leq \frac{4\theta(0)}{\pi^2 T \Delta f^2} \quad (13)$$

The interference is completely removed as  $T(\Delta f)^2 \rightarrow \infty$ .

## 2.4 Frequency Resolution

An important characteristics of a GTFR is the closeness at which two frequencies can be resolved. As we will show that both the DD and ZAM GTFR can display quite good frequency resolution properties.

Assume that the signal  $x(t)$  is as in (9) with  $X_1 = X_2 = X$ . We will evaluate the resolution measure

$$\mathcal{B}(t; T) = \max \left\{ \frac{C(t, (f_1 + f_2)/2; \rho)}{C(t, f_1; \rho)} \right\}.$$

We now compare the performance of the spectrogram, Wigner distribution, ZAM and DD GTFR's using Hanning windows in each case. For a Hanning window,  $\theta(u) = \cos^2(\pi u/2)$ .

First, consider the ZAM GTFR. From (10), we can write [11]

$$\begin{aligned} C(t, f; \theta) &= C_1^{(1)}(t, f; \theta) + C_2^{(1)}(t, f; \theta) + C_{12}^{(2)}(t, f; \theta) + C_{21}^{(2)}(t, f; \theta) \\ &= 2|X|^2 T \{ \text{Re}\{\Theta^{(1)}\{(f - f_1)T\}\} + \Theta^{(1)}\{(f - f_2)T\} \} \\ &+ \frac{\cos[2\pi(f_1 - f_2)t]}{\pi(f_1 - f_2)T} \text{Im}\{\Theta^{(2)}\{(f - f_2)T\} - \Theta^{(2)}\{(f - f_1)T\}\} \} \end{aligned}$$

Therefore,

$$\mathcal{B}_{ZAM}(t, T) = \max\{\mathcal{B}_{ZAM}^{(1)}, \mathcal{B}_{ZAM}^{(2)}\} \quad (14)$$

where

$$\mathcal{B}_{ZAM}^{(1)} = 2 \frac{\pi p \text{Re}\{\Theta^{(1)}(p/2)\} - \text{Im}\{\Theta^{(2)}(p/2)\}}{\pi p \text{Re}\{\Theta^{(1)}(0) + \Theta^{(1)}(p)\} + \text{Im}\{\Theta^{(2)}(0) + \Theta^{(2)}(p)\}}$$

$$\mathcal{B}_{ZAM}^{(2)} = 2 \frac{\pi p \text{Re}\{\Theta^{(1)}(p/2)\} + \text{Im}\{\Theta^{(2)}(p/2)\}}{\pi p \text{Re}\{\Theta^{(1)}(0) + \Theta^{(1)}(p)\} - \text{Im}\{\Theta^{(2)}(0) + \Theta^{(2)}(p)\}}$$

and  $p = (f_1 - f_2)T$ .

For the spectrogram with a Hanning window, the resolution measure is

$$\mathcal{B}_s(t; T) = \left[ \frac{2\text{Re}\{\Theta^{(2)}(p/2)\}}{\text{Re}\{\Theta^{(2)}(0)\} + \text{Re}\{\Theta^{(2)}(p)\}} \right]^2 \quad (15)$$

For the Wigner distribution, we have

$$\mathcal{B}_w(t; T) = \frac{1 + \text{sinc}(p)}{1 + 2\text{sinc}(p) + \text{sinc}(2p)} \quad (16)$$

Lastly, for the DD GTFR,

$$\mathcal{B}_{DD}(t, T) = \max\{\mathcal{B}_{DD}^{(1)}, \mathcal{B}_{DD}^{(2)}\} \quad (17)$$

where

$$\mathcal{B}_{DD}^{(1)} = \frac{4[\text{Re}\{\Theta^{(2)}(p/2)\}]^2}{[\text{Re}\{\Theta^{(2)}(0)\} + \text{Re}\{\Theta^{(2)}(p)\}]^2 - [\text{Im}\{\Theta^{(2)}(p)\}]^2} \quad (18)$$

and

$$\mathcal{B}_{DD}^{(2)} = \frac{-4\text{Im}\{\Theta^{(2)}(p/2)\}]^2}{[\text{Re}\{\Theta^{(2)}(0)\} - \text{Re}\{\Theta^{(2)}(p)\}]^2 - [\text{Im}\{\Theta^{(2)}(p)\}]^2} \quad (19)$$

Figure 7 shows the resolution measures of the spectrogram, Wigner distribution, ZAM and DD GTFR's rectangular and Hanning windows. Remarkably, the values for  $\mathcal{B}_s(t; T)$  are graphically indistinguishable from that for the double diamond  $\mathcal{B}_{DD}(t; T)$ . Note the different scales for the plot.

## 2.5 Time Resolution

An important characteristic of a TFR is its response to rapid nonstationarity. An indication of this property is the analysis of the TFR's response to a sinusoid whose frequency changes abruptly. We can denote such a signal by

$$x(t) = \begin{cases} X e^{j2\pi f_1 t} & ; t \leq 0 \\ X e^{j2\pi f_2 t} & ; t > 0 \end{cases}$$

The performance of a TFR in resolving this transition will be illustrated by the function

$$C(t; T) = \frac{C(t, f_2; \rho)}{C(T, f_2; \rho)}$$

For the rectangular windowed double diamond, this function is

$$\mathcal{C}_{DD}(t; T) = \begin{cases} (1 + \gamma)\{\gamma \text{sinc}(2\gamma p) + (1 - \gamma)\text{sinc}[2(1 - \gamma)p]\} \\ + \frac{1}{2}\{(1 - \gamma)^2 \text{sinc}^2[(1 - \gamma)p] \\ - \gamma^2 \text{sinc}^2(\gamma p) - \text{sinc}^2(\gamma p)\} & ; t \leq 0 \\ \gamma + (1 - \gamma)\text{sinc}[2(1 - \gamma)p] & ; t > 0 \end{cases}$$

where  $\gamma = t/T$ .

For the rectangular windowed ZAM GTFR, this function is

$$\mathcal{C}_{ZAM}(t; T) = \begin{cases} [\text{sinc}(p)]^2 - 2\gamma \text{sinc}(2p) - 2\gamma^2 [\text{sinc}(\gamma p)]^2 \\ + 2\gamma(1 + \gamma)\text{sinc}(2\gamma p) & ; t \leq 0 \\ 1 - (1 - \gamma)^2 \{1 - [\text{sinc}[(1 - \gamma)p]]^2\} & ; t > 0. \end{cases}$$

The corresponding functions for the Wigner distribution and spectrogram are, respectively,

$$\mathcal{C}_w(t; T) = \begin{cases} 2\gamma \text{sinc}(\gamma p) + [1 - \gamma]\text{sinc}[(1 - \gamma)p] & ; t \leq 0 \\ \gamma + [1 - \gamma]\text{sinc}[(1 - \gamma)p] & ; t > 0 \end{cases}$$

and

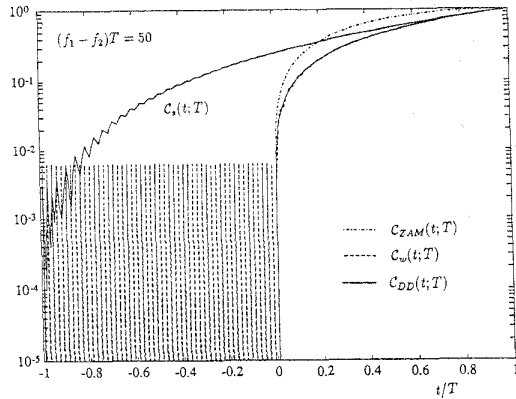


Figure 8: The response of an abrupt frequency transition from  $f_1$  to  $f_2$  monitored at  $f_2$  for the Wigner distribution, spectrogram, ZAM GTFR and DD GTFR for  $(f_1 - f_2)T = 50$ . The DD GTFR displays quite a good rise time without oscillation.

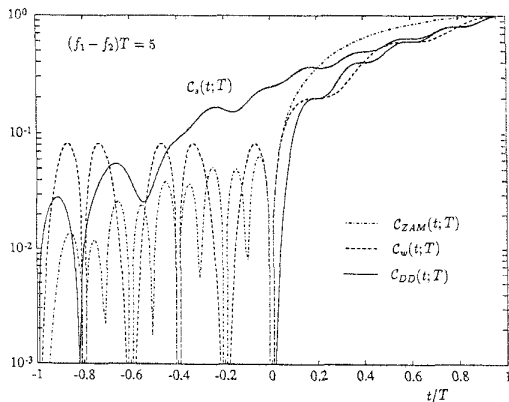


Figure 9: Same as the previous figure, except  $(f_1 - f_2)T = 5$ . The DD GTFR again displays quite a good rise time without oscillation.

$$C_s(t;T) = \frac{1}{4} \left[ (1 + \gamma)^2 + 2[1 - \gamma^2] \text{sinc}[2(1 - \gamma)p] + (1 - \gamma)^2 \{ \text{sinc}[(1 - \gamma)p] \}^2 \right]$$

Figure 8 and 9 show the response on frequency line  $f_2$  for four TFR's. Note that, in both figures, the DD GTFR response does not oscillate prior to the transition, yet displays quite a sharp temporal response. The plot in Figure 9 is redrawn at a different scale in Figure 10 to investigate leakage effects. The DD GTFR clearly has the best leakage property of those TFR's shown.

## 2.6 Noise Effects

A significant problem of the Wigner distribution is its high noise sensitivity. To compare the noise properties of TFR's, we assume that the signal under examination is corrupted by and zero mean wide sense stationary noise,  $n(t)$ , with autocorrelation

$$R(\tau) = E[n(s + \frac{\tau}{2})n^*(S - \frac{\tau}{2})] = \mathcal{N}_0 \delta(\tau) \quad (20)$$

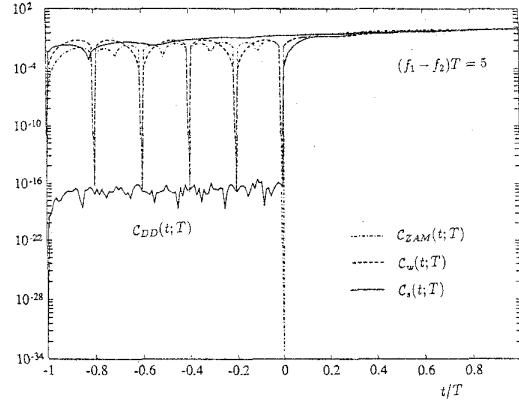


Figure 10: Same as the previous figure, except the scale has been changed to examine leakage. The DD GTFR has the best property in this regard.

where 'E' denotes the expectation operator. For a GTFR which satisfies the marginal constraints, the mean of the GTFR result is the sum of the value of the GTFR without noise and the spectral density of the noise [13, 14]. Such is the case for the CW GTFR and the Wigner distribution. Such is not the case for the DD or ZAM GTFR's. We can establish, rather, the following useful property.

**Property 2** Let the kernel,  $\hat{\phi}(t; \tau)$  be such that

$$\int_{-\infty}^{\infty} \hat{\phi}(t; 0) dt = 0 \quad (21)$$

Then, when a signal is corrupted by wide sense stationary noise, the resulting GTFR will be an unbiased estimate of the GTFR of the signal without noise.

A proof is in reference [11]. Since both the DD and ZAM GTFR pinch to zero at the origin of the  $(t, \tau)$  plane, they satisfy (21). Thus, in the presence of wide sense stationary white noise, the DD and ZAM GTFR's generates an unbiased estimate of the ZAM GTFR without noise. The unbiasedness, however, comes at the price of no longer being able to satisfy the instantaneous power marginal. In other words, unlike the Wigner distribution and CW GTFR, the integration of the ZAM GTFR over all frequency does not result in the instantaneous power of the signal [1].

## 3 Conclusion

We have investigated relative performance attributes of the ZAM and DD GTFR's. The DD GTFR appears to have some quite remarkable performance attributes. Further work is required to further define and understand the extent and limitations of some of these properties.

## Acknowledgements

We thank Hal Philipp of Philipp Technologies Corporation for his help and encouragement.

## References

- [1] L. Cohen, "Time-frequency distribution - a review," *Proceedings of the IEEE*, vol. 77, pp. 941-981, July 1989.
- [2] L. Cohen, "Generalized phase-space distribution function," *J. Math. Physics*, vol. 7, pp. 781-786, 1966.
- [3] H. Choi and W. J. Williams, "Improved time-frequency representation of multicomponent signal using exponential kernels," *IEEE Trans. on Acoustics, Speech, and Signal Processing*, vol. ASSP-17, pp. 862-871, June 1989.
- [4] W. J. Williams and J. Jeong, "New time-frequency distribution: theory and applications," in *Proceedings of International Conference on Circuits and Systems*, (Portland, Oregon), 1989.
- [5] L. E. Atlas, Y. Zhao, and R. J. Marks II, "Application of the generalized time-frequency representation to speech signal analysis," in *Proceedings of the IEEE Pacific Rim Conference on Communications, Computer and Signal Processing*, (Victoria, B. C. Canada), pp. 517-519, 1987.
- [6] L. E. Atlas, Y. Zhao, and R. J. Marks II, "The use of cone-shape kernels for generalized time-frequency representations of nonstationary signals," *IEEE Trans. on Acoustics, Speech, and Signal Processing*.
- [7] M. Born and P. Jordan, "Zur quantenmechanik," *Z. Phys.*, vol. 34, pp. 858-888, 1925.
- [8] W. Martin and P. Flandrin, "Wigner-ville spectral analysis of nonstationary processors," *IEEE Trans. on Acoustics, Speech, and Signal Processing*, vol. ASSP-33, pp. 1461-1470, Dec. 1985.
- [9] J. C. Andriux, M. R. Feix, G. Mourgues, P. Bertrand, B. Izrar, and V. T. Nguyen, "Optimum smoothing of the wigner-ville distribution," *IEEE Trans. on Acoustics, Speech, and Signal Processing*, vol. ASSP-35, pp. 764-769, June 1987.
- [10] L. E. Atlas, P. J. Loughlin, J. W. Pitton, and W. L. J. Fox, "Application of cone-shaped kernel time-frequency representations to speech and sonar analysis," in *Proceedings of International Symposium Signal Processing and Applications*, (Gold Coast, Australia), Aug. 27-31, 1990.
- [11] S. Oh and R. J. Marks II, "Some properties of the generalized time frequency representation with cone shaped kernel", submitted to *IEEE Transactions on Acoustics, Speech and Signal Processing*.
- [12] S. Oh and R. J. Marks II, L. E. Atlas and J. W. Pitton, "Kernel synthesis for generalized time-frequency distributions using the method of projection onto convex sets," in *Proceedings of SPIE Conference on Advanced Signal Processing, Algorithms, Architectures and Implementation*, (San Diego, California), 1990.
- [13] T. E. Posch, "Time-frequency distribution for a wide sense stationary random signal," in *Proceedings of International Conference on Circuits and Systems*, (Portland, Oregon), pp. 1235-1236, 1989.
- [14] T. E. Posch, "Time-frequency distribution for a wide-sense stationary random signal," *IEEE Trans. on Acoustics, Speech, and Signal Processing*, vol. 38, no. 4, pp. 725-727, 1990.
- [15] R. J. Marks II, *Shannon Sampling and Interpolation Theory*. New York: Springer-Verlag, 1991.
- [16] A. Ralston and P. Rabnowitz, *A First Course in Numerical Analysis, second Ed.* New York: Mc Graw Hill, 1978.

